

Counterflow-Induced Inverse Energy Cascade in Three-Dimensional Superfluid Turbulence

Juan Ignacio Polanco and Giorgio Krstulovic

*Université Côte d'Azur, Observatoire de la Côte d'Azur, CNRS, Laboratoire Lagrange,
Boulevard de l'Observatoire CS 34229 - F 06304 NICE Cedex 4, France*

Finite-temperature quantum turbulence is often described in terms of two immiscible fluids that can flow with a non-zero mean relative velocity. Such out-of-equilibrium state is known as counterflow superfluid turbulence. We report here the emergence of a counterflow-induced inverse energy cascade in three-dimensional superfluid flows by performing extensive numerical simulations of the Hall-Vinen-Bekarevich-Khalatnikov model. As the intensity of the mean counterflow is increased, an abrupt transition, from a fully three-dimensional turbulent flow to a quasi two-dimensional system exhibiting a split cascade, is observed. The findings of this work could motivate new experimental settings to study quasi two-dimensional superfluid turbulence in the bulk of three dimensional experiments. They might also find applications beyond superfluids in systems described by more than one fluid component.

Turbulence is an out-of-equilibrium state observed in fluids when a large scale separation exists between the forcing scale, at which the fluid is stirred, and the dissipation scales where energy is efficiently purged out from the system. As a result of the inherently non-linear dynamics of fluids, energy is transferred along scales. Such idea led Richardson to propose his cascade scenario, where in three-dimensional classical turbulence, energy is transferred towards small scales in a cascade process [1]. Such a *direct* cascade, i.e. with energy flowing from large to small scales, is ubiquitous in nature. It also takes place for instance in magnetohydrodynamic turbulence (e.g. in the solar wind [2]) and in quantum turbulence [3]. It was later realized by Kraichnan that, in two dimensions, due to the conservation of enstrophy (mean vorticity square), a different scenario takes place [4]. Energy flows towards large scales through an *inverse* cascade, whereas enstrophy flows toward small scales by a direct cascade. Such scenario has been confirmed experimentally and numerically (see [5] and references therein).

More complex systems, such as stratified rotating turbulence, magnetohydrodynamics with a strong background field and some decimated models of turbulence, might even present split cascades and transitions, where fluxes can change direction depending on some external parameters [6–9]. Similarly, thin layer flows, where one dimension is progressively squeezed, exhibit an abrupt transition from three to two dimensional phenomenology [10, 11]. More recently, such kind of abrupt transition has also been reported in numerical simulations of low-temperature superfluid turbulent flows [12].

Superfluids are peculiar types of fluids characterized by the complete absence of viscosity at low temperature and the presence of quantized vortices (filaments with a quantized circulation). At finite temperatures, such fluids are composed of two immiscible components: a superfluid with no viscosity, and a viscous normal fluid [13]. The latter is described by the Navier-Stokes equations. These two fluids are coupled through a mutual friction force

which arises from the scattering of thermal excitations on quantized vortices [13, 14]. The two-fluid description, originally proposed by Landau, enables the possibility of a turbulent state with no classical analogous, in which the mean relative velocity between these two components is non-zero. Such out-of-equilibrium state is known as *counterflow* turbulence and is typically produced by imposing a temperature gradient in a channel [3, 14]. Recent numerical studies of counterflow turbulence have shown a tendency of the system to develop large-scale quasi-two-dimensional structures [15, 16]. This observation suggests the possibility of a counterflow-induced inverse energy cascade in quantum turbulent flows.

In this Letter, we investigate the emergence of a split energy cascade in counterflow superfluid turbulence using direct numerical simulations of the coarse-grained Hall-Vinen-Bekarevich-Khalatnikov (HVBK) model. We show an abrupt transition from an isotropic 3D flow (in the absence of a mean counterflow) to a quasi-2D flow as the mean counterflow velocity is increased. In particular, for strong counterflow, we observe at large scales the Kolmogorov-Kraichnan phenomenology of two-dimensional turbulence. Such a large-scale manifestation is pure consequence of counterflow turbulence, and can thus be seen as a macroscopic manifestation of quantum mechanics.

At scales larger than the mean inter-vortex distance, finite-temperature superfluid helium can be described by the HVBK equations. In this framework, the motion of discrete quantum vortices is replaced by their effective coarse-grained dynamics, represented by a continuous superfluid velocity field. The turbulent velocity fluctuations \mathbf{v}_n and \mathbf{v}_s of the normal and superfluid components then follow two coupled Navier-Stokes equations [13, 15, 17, 18],

$$\frac{\partial \mathbf{v}_c}{\partial t} + (\mathbf{U}_c + \mathbf{v}_c) \cdot \nabla \mathbf{v}_c = -\frac{\nabla p_c}{\rho_c} + \nu_c \nabla^2 \mathbf{v}_c + \mathbf{f}_c + \boldsymbol{\varphi}_c, \quad (1)$$

$$\nabla \cdot \mathbf{v}_c = 0, \quad c \in \{n, s\} \quad (2)$$

where the subscript c identifies each component. The normal fluid viscosity is denoted by ν_n . The effective superfluid viscosity ν_s accounts for energy dissipation due to physics not resolved by the HVBK equations, including small-scale mutual friction, quantum vortex reconnections and Kelvin wave excitation [18, 19]. The respective densities of the normal and superfluid are ρ_n and ρ_s , and the total density of the fluid is $\rho = \rho_n + \rho_s$. The two fluids are stirred by independent zero-mean 3D Gaussian random forces $\boldsymbol{\varphi}_n$ and $\boldsymbol{\varphi}_s$ of equal variance σ_f^2 . In this model, a mean counterflow velocity $\mathbf{U}_{ns} = \mathbf{U}_n - \mathbf{U}_s$ is imposed by setting the respective mean velocities of each component, \mathbf{U}_n and \mathbf{U}_s . Despite \mathbf{U}_{ns} being a mean quantity, it cannot be removed with a Galilean transformation, unlike a constant mean flow in classical turbulence. The case of zero mean counterflow is known as *coflow* quantum turbulence.

The mutual friction forces are $\mathbf{f}_s = -(\rho_n/\rho_s)\mathbf{f}_n = \mathbf{f}_{ns}$, where \mathbf{f}_{ns} depends on $\mathbf{v}_{ns} = \mathbf{v}_n - \mathbf{v}_s$. In the simplest HVBK description, this coarse-grained mutual friction force reads $\mathbf{f}_{ns} = \alpha\Omega_0\mathbf{v}_{ns}$, where α is a temperature-dependent non-dimensional coefficient [19], and the mutual friction frequency Ω_0 is related to the density and polarization of quantum vortices. When vortex lines are randomly oriented, as is the case in coflowing quantum turbulence, this frequency may be estimated as $\Omega_0 \approx \sqrt{\langle|\boldsymbol{\omega}_s|^2\rangle}/2$ [20, 21], where $\boldsymbol{\omega}_s$ is the coarse-grained superfluid vorticity, and $\langle\cdot\rangle$ is an average over space. Under strong counterflow, the vortex orientation is anisotropic, and this expression may underestimate the actual friction. In this case, a common approach is to take Ω_0 as an external control parameter [15, 22]. Unless stated otherwise, the first estimation is used throughout this work.

We numerically solve Eqs. (1–2) using a standard fully parallelized pseudo-spectral solver in a cubic periodic box of size $L = 2\pi$ [23]. For the sake of simplicity, we only consider here the case of superfluid helium at $T = 1.9$ K, where the two fluid components have similar densities ($\rho_s/\rho_n = 1.35$) and viscosities ($\nu_s/\nu_n = 1.25$) [19, 24].

The total energy per unit volume of the system is $\rho E = \rho_n E_n + \rho_s E_s$, where $E_c = \langle|\mathbf{v}_c|^2\rangle/2$ is the turbulent kinetic energy associated to each component. We consider the energy spectra

$$E_c(k) = \frac{1}{2} \sum_{\mathbf{k} \leq |\mathbf{k}| < k+1} |\widehat{\mathbf{v}}_c(\mathbf{k})|^2 \quad \text{for } k \in \mathbb{Z}, c \in \{n, s\}, \quad (3)$$

where $\widehat{\mathbf{v}}_c(\mathbf{k})$ is the Fourier transform of \mathbf{v}_c , and \mathbf{k} its wave vector. The total energy spectrum is the weighted average $E(k) = [\rho_n E_n(k) + \rho_s E_s(k)]/\rho$. It quantifies the scale-by-scale repartition of turbulent kinetic energy of the fluid as a whole. The relative velocity spectrum $E_{ns}(k)$ is defined by replacing $\widehat{\mathbf{v}}_c$ with $\widehat{\mathbf{v}}_{ns}$.

A first simulation is performed using $N^3 = 1024^3$ collocation points, with independent steady 3D forcings $\boldsymbol{\varphi}_n$ and $\boldsymbol{\varphi}_s$ localized at the wave number $k_f = 15$. Initially, the two

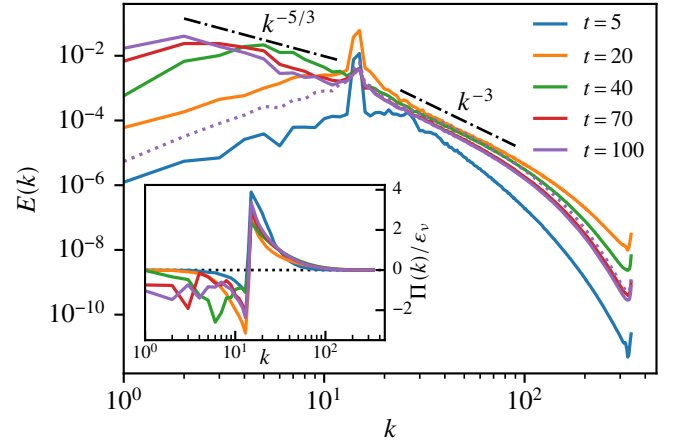


FIG. 1. Temporal evolution of the total energy spectrum under strong counterflow at $T = 1.9$ K. Dotted line: relative velocity spectrum $E_{ns}(k)$ at the final time. In the legend, times are scaled by the forcing time scale $t_f = (k_f \sigma_f)^{-1/2}$. Inset: normalized total energy flux. At the final time, the normal fluid Reynolds number is $\text{Re}_n = 159$.

components have no velocity fluctuations ($\mathbf{v}_n = \mathbf{v}_s = 0$). The imposed counterflow velocity, normalized by the forcing velocity $v_f = \sqrt{\sigma_f/k_f}$, is $\tilde{U}_{ns} \equiv U_{ns}/v_f = 40$. In Fig. 1, the time evolution of the total energy spectrum is shown. Over time, energy flows from k_f towards both the smallest and the largest scales of the system, suggesting the formation of a split cascade. Note that this behavior does not occur in classical three-dimensional turbulence, where a power-law spectrum k^n with $n \geq 1$, usually associated to thermalized modes, is observed at scales larger than the forcing one [25]. We have observed that both the normal and superfluid energy spectra follow the same trend as $E(k)$. In particular, since the two components are locked at large scales, the three spectra are almost identical for $k < k_f$. We have also verified that this phenomenon is robust if we turn off the forcing on the superfluid component, or if both forcings are applied at different scales.

In the HVBK system, energy is dissipated by the coarse-grained mutual friction force, by the kinematic viscosity ν_n of the normal fluid, and by the effective viscosity ν_s of the superfluid. It follows from Eq. (1) that

$$\frac{dE}{dt} = -(\varepsilon_\nu + \varepsilon_{MF}) + \mathcal{I}, \quad (4)$$

where $\rho\varepsilon_\nu = \rho_n\nu_n\langle|\boldsymbol{\omega}_n|^2\rangle + \rho_s\nu_s\langle|\boldsymbol{\omega}_s|^2\rangle$ is the small-scale viscous dissipation, $\rho\mathcal{I} = \rho_n\langle\mathbf{v}_n \cdot \boldsymbol{\varphi}_n\rangle + \rho_s\langle\mathbf{v}_s \cdot \boldsymbol{\varphi}_s\rangle$ is the power injected by the forcing, and $\varepsilon_{MF} = \Omega_{ns}\langle|\mathbf{v}_{ns}|^2\rangle$ is the dissipation by mutual friction, with $\Omega_{ns} = \alpha\rho_s\Omega_0/\rho$. Note that $E_{ns}(k)$ is directly related to the mutual friction dissipation as $\varepsilon_{MF} = 2\Omega_{ns}\sum_k E_{ns}(k)$, and thus characterizes the scale-by-scale contributions to ε_{MF} . Additionally, as customary in turbulence [1], one can define the energy flux across wave number k as $\Pi_c(k) = \langle\mathbf{v}_c^{<k} \cdot [\mathbf{v}_c \cdot \nabla \mathbf{v}_c]\rangle$, where $\mathbf{v}_c^{<k}$ is the low-pass filtered velocity field \mathbf{v}_c such

that $\hat{v}_c(\mathbf{k}) = 0$ for $|\mathbf{k}| > k$. The energy flux $\Pi_c(k)$ quantifies the non-linear transfer of energy from large scales (such that $|\mathbf{k}| \leq k$) to small scales ($|\mathbf{k}| > k$). The total energy flux $\Pi(k)$ is defined as the weighted average of the normal and superfluid contributions.

The inset of Fig. 1 shows the energy flux at different times. Notably, it is negative and relatively flat for $k < k_f$, indicating the presence of an inverse energy cascade. Conversely, it is positive for $k > k_f$ indicating also a transfer towards small scales. The direct cascade builds up rapidly, and has a scaling compatible with k^{-3} . In classical 2D turbulence, this scaling is associated to a constant enstrophy flux at small scales [4, 5, 26]. It has also been predicted theoretically in 2D flows with small-scale 3D perturbations [27]. Elucidating the origin of such scaling is out of the scope of this Letter, as we focus on the inverse energy cascade.

The build-up of the inverse cascade ($k < k_f$) is slower. As in 2D turbulence, a Kolmogorov $k^{-5/3}$ spectrum starts to develop at large scales. Due to the lack of a large-scale dissipation, energy accumulates at the largest scales, eventually leading to the formation of a condensate.

As suggested by the $E_{ns}(k)$ spectrum in Fig. 1 (dotted magenta line), the mutual friction dissipation is negligible at scales larger than the forcing, and thus the inverse cascade dynamics is expected to be similar to that of 2D turbulence. Namely, energy flows towards the largest scales with negligible loss due to mutual friction. This is not the case for the direct cascade, which coexists with a strong mutual friction dissipation. Hence, for any given $k > k_f$, a fraction of the energy flows towards smaller scales, while another part is locally dissipated by mutual friction. As a result, $\Pi(k)$ monotonically decreases for $k > k_f$, and an inertial range with a constant energy flux is never observed.

To characterize the effect of the Reynolds number and of the mutual friction coupling on the split cascade, we perform simulations at resolutions $N^3 = 512^3$ and 1024^3 with different viscosities ν_s and ν_n , while keeping their ratio $\nu_s/\nu_n = 1.25$ constant. The normal component Reynolds number is $Re_n = v_{rms}^{(n)}/(\nu_n k_f)$, with $v_{rms}^{(n)}$ the standard deviation of \mathbf{v}_n . The counterflow velocity is fixed at $\tilde{U}_{ns} = 40$. As shown in Fig. 2, the $k^{-5/3}$ scaling of the inverse cascade is already robust for moderately large Reynolds numbers, while the direct cascade tends to the k^{-3} scaling at increasing Re_n . Also included is a simulation (dotted lines) with a viscosity ratio $\nu_s/\nu_n = 0.25$ which also displays an inverse energy cascade. This suggests that the choice of effective superfluid viscosity has no influence on the large scale dynamics. Finally, we include a simulation (dashed lines) with an imposed mutual friction frequency Ω_0 that is 4 times larger than the one resulting from the ω_s -based estimate. The higher coupling between the two components has no apparent influence on the inverse cascade, while at the small scales, it further suppresses the velocity fluctuations. Neverthe-

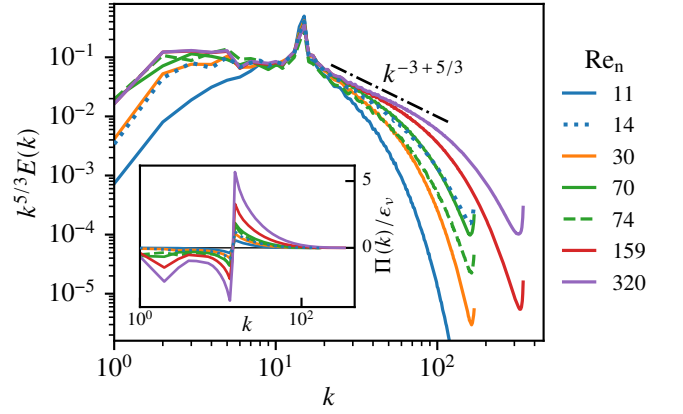


FIG. 2. Compensated total energy spectrum under strong counterflow at $T = 1.9$ K for different Reynolds numbers. Counterflow values are kept the same, $\tilde{U}_{ns} = 40$, across all simulations. Solid lines, $\nu_s/\nu_n = 1.25$ and $\Omega_0^2 = \langle |\omega_s|^2 \rangle / 2$; dotted line, viscosity ratio $\nu_s/\nu_n = 0.25$ (low ν_s case); dashed line, externally imposed Ω_0 (high mutual friction case). Inset: total energy flux $\Pi(k)/\epsilon_\nu$. Spectra and fluxes are averaged over $\Delta t = 30 t_f$.

less, as confirmed by the energy fluxes (inset of Fig. 2), the double cascade scenario remains mostly unchanged when the coupling is stronger.

We now proceed to study the transition from the co-flowing turbulence with no inverse cascade to the counterflow-induced double cascade scenario. For this, we perform a parametric analysis by varying the counterflow velocity U_{ns} while setting constant forcing and mutual friction parameters. The simulations are performed at resolutions $N^3 = 128^3$ and 256^3 . We now include in Eq. (1) a large scale dissipation term to obtain a statistically steady state. Moreover, to increase the span of the direct and inverse inertial ranges, the dissipations are strongly localized in wave number space by imposing hypofriction and hyperviscosity mechanisms [5]. These modifications are obtained by replacing the viscous dissipative terms in Eq. (1) with $-\nu'(-\nabla^2)^4 + \mu'(-\nabla^2)^{-4}]v_c$. For simplicity, the two fluid components are given the same values of ν' and μ' . Finally, similar to other studies of transition to 2D turbulence [10, 28], a 2D forcing scheme is introduced, in which the external forces φ_c are orthogonal to the mean counterflow and do not vary in that direction (i.e. $U_{ns} \cdot \varphi_c = U_{ns} \cdot \nabla \varphi_c = 0$).

The energy balance (4) now writes $dE/dt = -(\epsilon_\mu + \epsilon_\nu + \epsilon_{MF}) + \mathcal{I}$, with ϵ_μ and ϵ_ν the large and small-scale dissipations respectively associated to the hypofriction and hyperviscous terms. We quantify the strength of the inverse energy cascade by the relative large-scale dissipation

$$Q_\mu = \frac{\epsilon_\mu}{\epsilon_\nu + \epsilon_\mu}. \quad (5)$$

Note that, in contrast to previous studies [28], here the

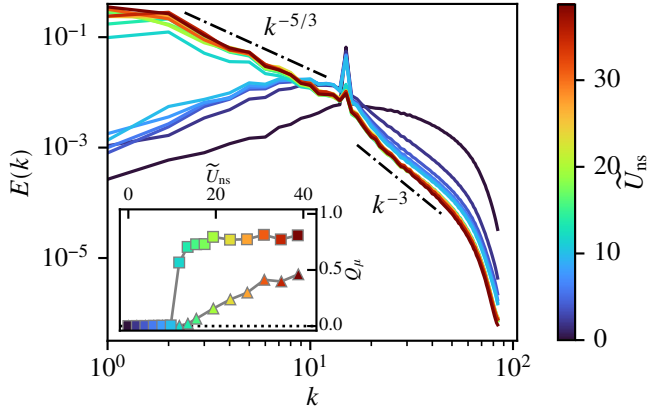


FIG. 3. Total energy spectrum for different counterflow velocities \tilde{U}_{ns} . Simulations are performed with a 2D forcing scheme, and include hypofriction and hyperviscosity terms (see text for details). Inset: relative large-scale dissipation Q_μ as a function of counterflow velocity, for 2D (squares) and 3D (triangles) forcing schemes. The forcing parameters (k_f, σ_f) are the same across all simulations.

denominator is not the injected power \mathcal{I} . This choice is made because the injected energy is mostly dissipated locally (in Fourier space) at the forcing scale by mutual friction (as suggested by the E_{ns} spectrum in Fig. 1, peaked at $k = k_f$).

The variation of the steady-state energy spectrum $E(k)$ with the imposed counterflow velocity U_{ns} is shown in Fig. 3 for a set of simulations with $N^3 = 256^3$. An abrupt transition is observed, from the absence of an inverse cascade at low U_{ns} , to a double cascade scenario with power laws characteristic of 2D turbulence at large U_{ns} . In the latter case, the inertial ranges are equivalent to those observed in higher-resolution simulations (Figs. 1 and 2), suggesting that the double cascade is not affected by the dissipation mechanisms at large and small scales. The dependence of Q_μ with \tilde{U}_{ns} (inset of Fig. 3), including for the sake of completeness the case of a 3D forcing scheme, confirms the appearance of an inverse energy cascade at a critical value of the counterflow velocity \tilde{U}_{ns}^* . Remarkably, the transition is much more abrupt when the forcing is two-dimensional than with the original three-dimensional scheme, even though the value of \tilde{U}_{ns}^* remains almost unchanged.

From dimensional analysis, the critical counterflow velocity U_{ns}^* can be expected to depend on the normalized forcing wave number k_f/k_L (where $k_L = 2\pi/L$), and on the non-dimensional mutual friction intensity $\tilde{\Omega}_{\text{ns}} = \Omega_{\text{ns}}/(k_f\sigma_f)^{1/2}$. Empirically, from multiple sets of simulations using different forcing and mutual friction parameters, we find the relation $\tilde{U}_{\text{ns}}^* = C \tilde{\Omega}_{\text{ns}}^{1/2} k_f/k_L$, where C is a non-dimensional constant. In terms of dimensional variables, this scaling becomes $U_{\text{ns}}^* \sim \sqrt{v_f \Omega_{\text{ns}}/k_f} (k_f/k_L)$. Note however, that this is an asymptotic formula which assumes that Ω_{ns} is sufficiently large, as for $\Omega_{\text{ns}} = 0$ the

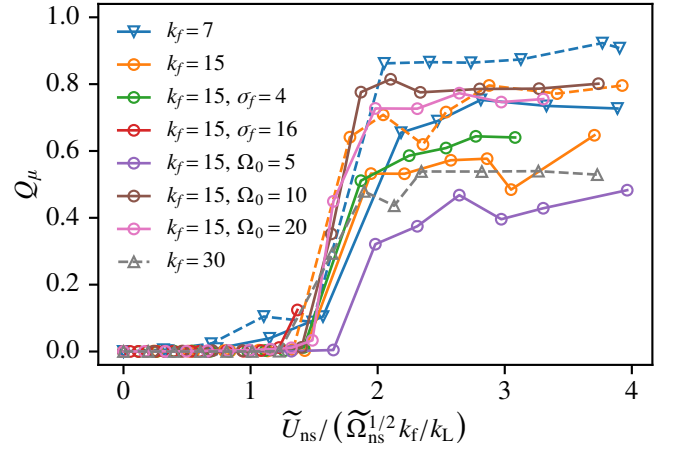


FIG. 4. Dissipation ratio as a function of the normalized counterflow velocity, for different forcing and mutual friction parameters. In all cases a 2D forcing scheme is used. Each marker corresponds to a single simulation. Resolutions are $N^3 = 128^3$ (solid lines) and 256^3 (dashed lines), with dissipative wave numbers of $k_\eta \approx 100$ and $k_\eta \approx 200$, respectively. Unless stated otherwise in the legend, the mutual friction frequency is $\Omega_0 = \sqrt{\langle |\omega_s|^2 \rangle}/2$ and the numerical value of the forcing intensity is $\sigma_f = 1$.

two fluids are uncoupled and no transition can be observed. Figure 4 displays the dissipation ratio Q_μ as a function of the counterflow velocity scaled according to the above empirical relation, for different values of the parameters. All simulations invariably display an abrupt transition towards a double cascade scenario at nearly the same scaled counterflow velocity, which corresponds to a non-dimensional constant $C \approx 1.5$. Note that we also present simulations with different values of the small-scale dissipative wavenumber k_η , validating the previous scaling. A theoretical explanation, and further verification of this empirical law, are out of the scope of this Letter.

We have shown clear evidence of an inverse energy cascade emerging in finite-temperature quantum turbulence under strong counterflow. Although described by coarse-grained fluid type equations, this phenomenon can be seen as a large scale manifestation of quantum mechanics. Indeed, it originates from the presence of a counterflow and the coupling between the two fluid components due to mutual friction, two physical phenomena that arise from quantum mechanical effects.

The appearance of an inverse cascade and the strong bidimensionalization suggest the possibility of using strong counterflow to produce (quasi-)two-dimensional turbulent flows in the bulk of three-dimensional experiments. Such experiments may be easier to realize than those performed in thin superfluid helium films [13, 29, 30]. From Fig. 2, we note that the Reynolds numbers needed to trigger the inverse cascade are relatively low. Therefore, an inverse energy cascade should be realizable for instance in superfluid experiments with moving or os-

cillating objects [31, 32], provided the experiments are performed over sufficiently long times, and that some scale separation exists between the object size and the container. Such object should move fast enough to ensure a Reynolds number of order $Re \sim 100$ (see Fig. 2). This is not very challenging for current experiments, and is low enough for the critical counterflow velocity to remain achievable (about 10–15 times the velocity of the object, see inset of Fig. 3).

In this Letter we have only reported the case of superfluid helium at $T = 1.9\text{ K}$, where the normal and superfluid densities are similar. At different temperatures, but still within the range of applicability of the HVBK model, the situation might be slightly more complex but the abrupt appearance of an inverse cascade remains unchanged (data not shown). This will be reported in a future work. Moreover, note that the large and small scale dissipation mechanisms have no influence on the emergence of the inverse cascade, making this finding universal.

Finally, we would like to remark that the results of this Letter might find applications in systems which are not related to superfluid helium, but whose physics is described by the presence of two or more fluid components. This is the case for instance of partially-ionized magnetohydrodynamics occurring in the upper atmospheres of hot Jupiters and in the interior of Gas Giant Planets [33, 34]. In such systems, in addition to the induction equation for the magnetic field, the fluid components are described by equations strongly resembling the HVBK model. However, since some components are charged, the components are also coupled to the magnetic field through the Lorenz force. It will be then of natural interest, to investigate the consequences of strong counterflow in the physics of planetary science and other multi-component fluid systems.

The authors thank U. Giurato and N. Müller for fruitful discussions. This work was supported by the Agence Nationale de la Recherche through the project GIANTE ANR-18-CE30-0020-01. GK was also supported by the Simons Foundation Collaboration grant “Wave Turbulence” (Award ID 651471). This work was granted access to the HPC resources of CINES and IDRIS under the allocation 2019-A0072A11003 made by GENCI. Computations were also carried out at the Mésocentre SIGAMM hosted at the Observatoire de la Côte d’Azur.

[1] U. Frisch, *Turbulence: The Legacy of A.N. Kolmogorov*, 1st ed. (Cambridge University Press, 1995).
 [2] F. Sagraoui, M. L. Goldstein, G. Belmont, P. Canu, and L. Rezeau, Phys. Rev. Lett. **105**, 131101 (2010).
 [3] C. F. Barenghi, L. Skrbek, and K. R. Sreenivasan, Proc. Natl. Acad. Sci. **111**, 4647 (2014).

[4] R. H. Kraichnan, Phys. Fluids **10**, 1417 (1967).
 [5] G. Boffetta and R. E. Ecke, Annu. Rev. Fluid Mech. **44**, 427 (2012).
 [6] A. Sen, P. D. Mininni, D. Rosenberg, and A. Pouquet, Phys. Rev. E **86**, 036319 (2012).
 [7] E. Deusebio, G. Boffetta, E. Lindborg, and S. Musacchio, Phys. Rev. E **90**, 023005 (2014).
 [8] K. Seshasayanan, S. J. Benavides, and A. Alexakis, Phys. Rev. E **90**, 051003(R) (2014).
 [9] L. Biferale, S. Musacchio, and F. Toschi, Phys. Rev. Lett. **108**, 164501 (2012).
 [10] A. Celani, S. Musacchio, and D. Vincenzi, Phys. Rev. Lett. **104**, 184506 (2010).
 [11] S. Musacchio and G. Boffetta, Phys. Fluids **29**, 111106 (2017).
 [12] N. P. Müller, M.-E. Brachet, A. Alexakis, and P. D. Mininni, Phys. Rev. Lett. **124**, 134501 (2020).
 [13] R. J. Donnelly, *Quantized Vortices in Helium II* (Cambridge University Press, 1991).
 [14] W. F. Vinen and D. Shoenberg, Proc. R. Soc. Lond. A **240**, 114 (1957).
 [15] L. Biferale, D. Khomenko, V. L’vov, A. Pomyalov, I. Procaccia, and G. Sahoo, Phys. Rev. Lett. **122**, 144501 (2019).
 [16] J. I. Polanco and G. Krstulovic, Phys. Rev. Fluids **5**, 032601 (2020).
 [17] P.-E. Roche, C. F. Barenghi, and E. Lévéque, EPL Europhys. Lett. **87**, 54006 (2009).
 [18] L. Boué, V. S. L’vov, Y. Nagar, S. V. Nazarenko, A. Pomyalov, and I. Procaccia, Phys. Rev. B **91**, 144501 (2015).
 [19] W. F. Vinen and J. J. Niemela, J. Low Temp. Phys. **128**, 167 (2002).
 [20] V. S. L’vov, S. V. Nazarenko, and L. Skrbek, J. Low Temp. Phys. **145**, 125 (2006).
 [21] L. Biferale, D. Khomenko, V. L’vov, A. Pomyalov, I. Procaccia, and G. Sahoo, Phys. Rev. Fluids **3**, 024605 (2018).
 [22] D. Khomenko, V. S. L’vov, A. Pomyalov, and I. Procaccia, Phys. Rev. B **93**, 014516 (2016).
 [23] H. Homann, O. Kamps, R. Friedrich, and R. Grauer, New J. Phys. **11**, 073020 (2009).
 [24] R. J. Donnelly and C. F. Barenghi, J. Phys. Chem. Ref. Data **27**, 1217 (1998).
 [25] A. Alexakis and M.-E. Brachet, J. Fluid Mech. **872**, 594 (2019).
 [26] G. K. Batchelor, Phys. Fluids **12**, II (1969).
 [27] L. Moriconi, Phys. Rev. E **54**, 1550 (1996).
 [28] A. Alexakis and L. Biferale, Phys. Rep. **767-769**, 1 (2018).
 [29] G. I. Harris, D. L. McAuslan, E. Sheridan, Y. Sachkou, C. Baker, and W. P. Bowen, Nature Phys **12**, 788 (2016).
 [30] D. L. McAuslan, G. I. Harris, C. Baker, Y. Sachkou, X. He, E. Sheridan, and W. P. Bowen, Phys. Rev. X **6**, 021012 (2016).
 [31] D. Duda, P. Švančara, M. La Mantia, M. Rotter, and L. Skrbek, Phys. Rev. B **92**, 064519 (2015).
 [32] P. Švančara and M. La Mantia, J. Fluid Mech. **832**, 578 (2017).
 [33] T. V. Zaqarashvili, M. L. Khodachenko, and H. O. Rucker, A&A **529**, A82 (2011).
 [34] S. J. Benavides and G. R. Flierl, J. Fluid Mech. **900**, A28 (2020).